

# CMM3 Group Design Project

Project Title: Modelling the suspension system of a Honda PCX 125 scooter

Group Number: Group 2

GitHub Repository URL: <https://github.com/Lukas-234/Motorbike-suspension-model>

## Group Member Contributions:

Each group member should list 2–3 bullet points summarising their main contributions (technical, organisational, or collaborative).

Name	Student ID	Main Contributions
Lukas Frankholz	S2543797	<ul style="list-style-type: none"><li>- Created the interpolation code</li><li>- Converted geographical coordinates into differences in distances between points</li><li>- Wrote section 3.3 on the report</li></ul>
Dylan Thies	S2534867	<ul style="list-style-type: none"><li>- Collaborated on the root finding code and logic</li><li>- Supported the mathematical modelling of the system</li><li>- Supported in the formatting and specifications of what to include in the report</li><li>- Collaborated on section 3.2 in the report (root finding)</li></ul>
Kitty Kay	s2623820	<ul style="list-style-type: none"><li>- Collaborated on the ODE code</li><li>- Collaborated on the writing of numerical methods section 3.4 of the report</li><li>- Wrote the references section of the report</li></ul>
Caleb Murdock	s2575794	<ul style="list-style-type: none"><li>- Collaborated on the root finding code and logic</li><li>- Collaborated to bring the numerical methods together</li><li>- Supported in the maths modelling and writing numerical methods</li><li>- Collaborated on section 3.2 in the report (root finding)</li></ul>
Camille Alldread	s2626210	<ul style="list-style-type: none"><li>- Collaborated on the ODE code</li><li>- Collaborated on merging the different codes together such as interpolation and ODE</li><li>- Collaborated on the writing of numerical methods section 3.4 on the report</li></ul>

## Summary of Group Work

Our group worked extremely well together on all aspects of the project. We had an average of 2 meetings outside of the scheduled Wednesday seminar. Teams as well as WhatsApp was very frequently used to facilitate group communications and meeting times. In terms of collaborative coding, our main system was pair programming sessions coupled with many commit changes in the different folders. These commits were always communicated via WhatsApp to ensure clarity of what is going on at each stage of the code development. We used a GitHub repository to upload and review code at each stage of the design process. At each meeting we would review everyone's code as a group to ensure everyone was up to date and quality and formatting was consistent. We also took minutes during each session to summarise what had been done and clarify what actions needed to be taken before the next meeting. This helped us to stay organised and break the tasks down effectively. The coding for the numerical methods was split

into three groups. One person wrote the interpolation code, while the ODEs and Root Finding methods were written by groups of 2. However, all aspects of the code were peer reviewed outside of the designated groups. The project report was written in a collaborative setting in person, with all members contributing effectively. The group was very open to helping each other when in need of support for learning, which meant members helped teach other in areas of lack of understanding.

### **Evidence of group work**

Number of GitHub commits: 133 total

Initially, each subgroup worked independently to research and develop their understanding of their designated section. As the development of the model moved forward, we slowly started integrating our knowledge and sections together until we finally fully came together and worked to merge each section and run the code smoothly, as well as write the report all together. This was all done in person as we felt this is where we communicated the best and had the highest level of productivity.

We did most of our group work and coding together during frequent in person meetings. Meeting summaries can be found within our Teams channel as well as meetings that were scheduled. Examples of review can also be found within some of the files on teams, either in meeting summaries or updates.

### **Generative AI Use Declaration**

Please check the latest University of Edinburgh guidance on generative AI usage - <https://information-services.ed.ac.uk/computing/comms-and-collab/elm/guidance-for-working-with-generative-ai>.

*AI Statement - "Academic integrity is an underlying principle of research and academic practice. All submitted work is expected to be your own. AI tools (e.g., ELM) should not be used to generate content for this assessment. However, you are allowed to use these tools to identify ideas, key themes, and plan your assessment. You may also use it to improve the clarity of your writing. If you use AI software, you must acknowledge its use in your submission."*

Please list below the Generative AI models used in your project:

- ChatGPT, Gemini

Uses of Generative AI:

- Brainstorming/outlining
- Concept clarification
- Grammar/spell-check
- Code suggestions/debug hints/tests
- Reference re-formatting
- Code structures
- Source finding

# Modelling the Suspension System of a Honda PCX125 Scooter

**What is the optimal spring stiffness and damping coefficient to maximise rider comfort on a Honda PCX125 Scooter?**

## 1.0 Introduction



Figure 1- image of Honda PCX125 Scooter [1]

We identified that a major issue when riding a motorcycle on roads is the comfort of the driver. Factors such as weather conditions or the profile of the roads majorly affect how often a person may ride. Our focus is to mitigate the discomfort the rider may feel due to the profiles of various road types. This may encourage the use of motorcycles compared to cars, which in turn will reduce the vast amount of fuel that is used each day. This reduction in fuel will therefore reduce greenhouse gas emissions [2].

Our project's aim is to focus on the comfort of a rider on a Honda PCX125 scooter. We have defined comfort as vertical acceleration as per BS ISO 2631-1:1997 [3], which states the maximum comfortable vertical acceleration levels for a driver. Our end goal of the project is to determine what spring stiffness ( $k_s$ ) and damping coefficient ( $c_0$ ) should be applied to stay within this acceptable vertical acceleration range throughout.

The reasoning behind this specific bike is that it is the most sold bike in the UK for 2024-2025 [4]; this leads us to believe that our system will apply to the largest number of people. Our model is based on road profile data from multiple roads around Edinburgh such as the Royal Mile, Pleasance Road, A701 Liberton Road, Queens Drive, the M8 to Glasgow, the M90 to Perth and the Edinburgh City Bypass. We selected the Edinburgh area as this is the most relevant to us as students at the University but also as it gives a vast range of road behaviours such as large hills, smooth road surfaces, speed bumps, and cobble stones. This will lead to an accurate model which tackles a variety of conditions and can be applied to real-world situations.

## 2.0 System Overview

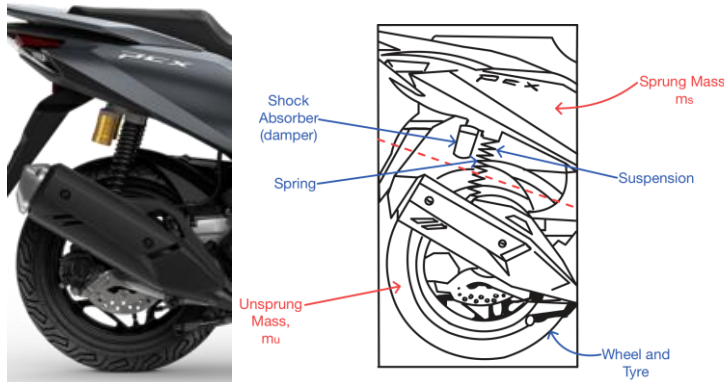


Figure 2 – Left: cropped image of Figure 1 to show rear suspension system.  
Right: diagram of rear suspension labelled with key parts.

Figure 2 (Left) demonstrates the physical set-up of the Honda PCX125 Scooter, specifically the rear wheel suspension system. The physical system is comprised of a wheel and tyre (unsprung mass,  $m_u$ ), a spring, a damper and the mass of the bike acting on the rear (sprung mass,  $m_s$ ). As seen in Figure 2 (Right), we simplified this image to the key parts such as the sprung mass, suspension, wheel, and tyre, which then can be further analysed to create the free body diagram as seen on the next page.

The key inputs for this system include the road profile data as vertical displacement ( $x_r(t)$ ), the sprung mass ( $m_s$ ), the unsprung mass ( $m_u$ ), tyre stiffness ( $k_t$ ) and the target natural frequency range of the springs. Key outputs for this system include spring stiffness ( $k_s$ ), damping coefficient ( $c_0$ ), vertical instantaneous and weighted accelerations of the sprung mass, and comfortability of the rider. Physical principles involved within our model include Newton's second law ( $F = ma$ ), Hooke's law ( $F = kx$ ), viscous damping ( $F = c\dot{x}$ ), static equilibrium (spring forces balance weight), energy conservation (kinetic, potential and dissipated energy balance) and linearity (proportionality between forces and displacements).

## 3.0 Mathematical Modelling and Numerical Methods

### 3.1 Mathematical Formulation

For this system we chose to analyse the rear suspension as this is where a larger percentage of the mass acts [5], in doing so we took the average mass of an adult [6], added this to the mass of the Honda PCX125 scooter [1] and took away 2 times the mass of a wheel plus the tyre [1]. We then found the capacity of the fuel tank of this bike [1] and density of unleaded petrol [7] and multiplied to find the mass of the fuel which was then added to the total mass of the bike. From this we multiplied by the percentage of the mass that acts on the rear suspension [5], this gave the sprung mass. The mass of the wheel and tyre as previously stated is the unsprung mass.

#### Simplified Diagram of System

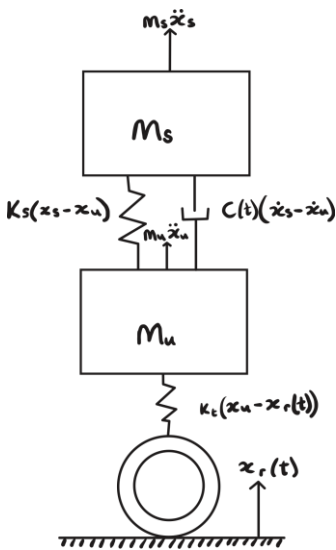


Figure 3 – Simplified diagram of the system.

#### Governing Equations

The following equations were obtained using the same logic as seen in “Engineering Vibration”, Inman, D.J. (2013) [8] and “Engineering Vibration Analysis with Application to Control Systems”, Beards, C. (1995) [9].

#### Sprung Mass ( $m_s$ ) + Unsprung Mass ( $m_u$ ):

$$m_s \ddot{x}_s + c_0(t)(\dot{x}_s - \dot{x}_u) + k_s(x_s - x_u) = F(t)$$

$$m_u \ddot{x}_u - c_0(t)(\dot{x}_s - \dot{x}_u) - k_s(x_s - x_u) + k_t(x_u - x_r(t)) = G(t)$$

#### System in Matrix Form

$$M\ddot{x} + C\dot{x} + Kx = 0$$

$$\text{where } x = \begin{bmatrix} x_s \\ x_u \end{bmatrix}, M = \begin{bmatrix} m_s & 0 \\ 0 & m_u \end{bmatrix}, C = \begin{bmatrix} c_0 & -c_0 \\ -c_0 & c_0 \end{bmatrix}, K = \begin{bmatrix} k_s & -k_s \\ -k_s & k_s + k_t \end{bmatrix}$$

#### State-Space Matrix (using System Matrix)

$$\dot{z} = \begin{bmatrix} 0 & I \\ -M^{-1}K & -M^{-1}C \end{bmatrix} z, \text{ where the matrix can be written as "A"}$$

#### Generalised Eigenvalue Problems (undamped and damped)

$$K\phi = \omega^2 M\phi, \quad \lambda v = Av$$

#### Varying Damping Coefficients (C(t)):

$$c_0(t) = c_0(1 + \alpha \sin(2\pi ft)) \quad \text{Where:}$$

$\alpha$  = variation due to environmental changes

$f$  = frequency of variation of damping coefficient

$c_0$  = damping coefficient

#### Residual Functions

$$f(k_s) - f_{target} = 0 \text{ and } \zeta(k_{s,optimal}, c_s) - \zeta_{target} = 0$$

#### Assumptions

- 1) Mass of rider and bike is a lumped mass, ensuring the system has 2 degrees of freedom.
- 2) Constant horizontal velocity of the bike (speed limit of each road respectively) which allows the road input to be defined purely as a function of distance, and conversion to the time domain through using the horizontal velocity.
- 3) Model is based on rear wheel, as this is where the majority of the weight acts in the real model so will dominate comfort.
- 4) Suspension is assumed to be vertically above the wheel allowing the system to remain with 2 degrees of freedom.
- 5) The sprung mass includes the masses of bike and rider acting on the rear wheel; proportional to the rear weight distribution [5]. This ensures the model reflects the actual static load carried by the rear suspension.
- 6) The unsprung mass includes the masses of the rear wheel and tyre.
- 7) Tyre modelled as a spring with specific stiffness, since tyres exhibit properties similar to springs.
- 8) No tyre slipping, the results of tyre slipping would mean that the distance travelled by the system would not match the road profile.
- 9) No losses due to wind resistance and friction; vertical displacement is directly proportional to acceleration. This ensures horizontal velocity is constant.
- 10) Mass of the system is modelled as constant (changes due to fuel use are negligible).
- 11) System is in static equilibrium when vertical displacement is equal to zero. Gravitational forces are already balanced by the spring pre-loading, simplifying the equations to only model deviation from the normal rider height.

### **3.2 Root Finding**

The goal of the root-finding was to determine the corresponding stiffness for a target natural frequency, as well as the corresponding damping coefficient for a target modal damping ratio, typical natural frequencies and a modal damping ratio for a motorcycle that optimizes comfort were found to be  $\zeta = 0.2$  [10] and in the range 1-1.6 Hz[11]. Accordingly, we targeted natural frequencies within this range in increments of 0.05 Hz. The residual functions which govern our system are non-linear because they depend on the 2-DOF eigenvalues and the ratio of their real and imaginary parts used to compute damping. As a result, computing their derivatives analytically would be much more complex, and computationally expensive particularly because mode tracking would be required. Over the design range the function is smooth and monotonic. The secant method is well-suited for this problem as it is derivative-free and converges efficiently for smooth and monotonic functions, offering an excellent balance between robustness and computational efficiency. We considered Newton-Raphson and bisection, however NR required derivatives that were slow and complex to compute and bisection resulted in a slower convergence.

To find the roots of our residual functions, the Secant technique uses two previous points in the graph to estimate the slope rather than the derivative (Newton-Raphson). The update is given by:

$$x_{n+1} = x_n - f(x_n) \frac{x_n - x_{n-1}}{f(x_n) - f(x_{n-1})}$$

Secant approximates the slope of the function using a line through the two most recent points, and it only requires one new function evaluation per iteration of the technique. For smooth functions like our residuals, convergence is typically achieved in only a few iterations.

The Secant method was applied twice in our model to solve two nonlinear equations arising from our 2-DOF system. First, it was used to identify the spring stiffness of the suspension that satisfies our frequency residual equation. At each iteration, the trial spring stiffness was inserted into the stiffness matrix, the generalised eigenvalue problem was solved, and the ride mode was identified by selecting the eigenvector with the highest sprung-mass participation. With the spring stiffness fixed, the same approach was applied to find the damping coefficient. Each secant iteration updated the damping coefficient, rebuilt the state-space matrix, extracted complex eigenvalues and calculated the corresponding modal damping ratio. In both cases, the roots converged in only a few iterations, and the resulting values were confirmed to lie within realistic ranges for motorcycle rear suspensions.

### **3.3 Interpolation/ Data Processing**

The raw data used in this project consisted of latitude and longitude values with a given altitude. Thus, the goal of the interpolation and data processing was to first convert these values into displacement-time values and interpolate between those values to get a smooth and continuous graph. To convert from degrees into meters, a factor of 111 139 [12] was applied to all latitude and longitude values, then after applying the Pythagorean Theorem, a distance between all points was calculated. Dividing the distance by a velocity in m/s led time values to be obtained. Finally, by subtracting the lowest altitude value from each altitude value, a displacement from the lowest point was found. Interpolation between all data points was done using spline interpolation. Spline interpolation involves fitting a cubic polynomial between each point. This will create a smooth curve between all data points. By importing “interpolate” from “scipy” in python, then using “`interpolate.splrep`”, a spline is calculated. Following this, “`interpolate.splev`” will evaluate the spline at specific points. Within the “`splrep`” function exists a value “`s`” which states how close the interpolation follows the data points. Higher `s` values will result in greater smoothing, while lower `s` values will follow the data points more closely. A higher “`s`” value proved to be valid for the higher speed roads as it filtered out the noise to create a low frequency road profile. This is what would be expected from a suspension system travelling at high speeds on a motorway, thus validating the interpolation of the system. Other roads utilized a lower “`s`” value given the lack of noise.

### **3.4 ODEs**

The goal of the simulation was to evaluate vertical acceleration against the BS ISO 2631-2:1997 comfort standards [3]. The governing equations were derived from the simplified diagram of the system (Figure 3). We rearranged the equations of motion to define acceleration for each mass in terms of displacement, velocity, and system coefficients. To prepare the model for the numerical solver, these second-order differential equations were rearranged to get acceleration in terms of velocity, displacement and system parameters. We assumed the system is in static equilibrium at zero vertical displacement; consequently, equilibrium restoring forces – such as weight and static spring force – were ignored.

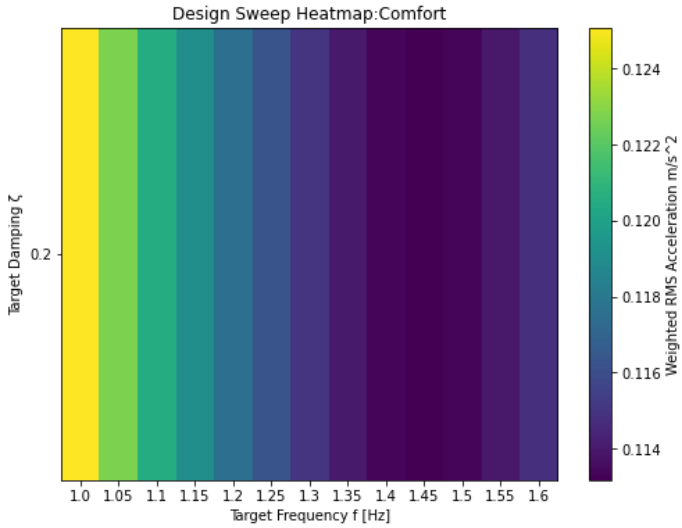
To solve this initial value problem, we utilized the `solve_ivp` function with the RK45 method. This is an adaptive implementation of the fourth-order Runge-Kutta (RK4) algorithm. We selected RK4 over simpler methods, such as Euler, based on accuracy requirements. Lecture analysis demonstrates that Euler approximations can introduce significant error (up to 5% in basic exponential decay models) unless extremely small steps are used [13]. In contrast, RK4 achieves high accuracy without requiring the computation of analytical higher-order derivatives. Theoretically, RK4 calculates the next value in the system ( $y_{i+1}$ ) by taking a weighted average of four different slope estimates calculated over the time step  $h$  [13]. These slopes are calculated at the start ( $k_1$ ), the midpoint ( $k_2$ ,  $k_3$ ), and the end ( $k_4$ ) of the interval. This method was chosen because it achieves high accuracy without needing higher-order derivatives [13], and the RK45 implementation specifically adapts the step size according to the data. This allows for easy scalability and accounts for sharp changes in acceleration as the system is not strongly stiff. For these reasons, RK45 is a widely used and appropriate method within time-domain vehicle vibration simulations.

The interpolated road profile served as the forcing function input to the solver. Post-processing was required to verify the solution against the "comfortable" boundaries defined in BS ISO 2631-1:1997 [3]. As raw instantaneous acceleration is not directly comparable to these standards, we applied a 'Wk filter' assisted by the methodology of a parallel study [14]. First, the acceleration power spectral density (PSD) was computed and divided into third octave bands, and the rms acceleration in each band calculated. The rms values were then weighted and recombined according to 'Wk' of Table 3 in BS ISO 2631-1:1997 [3]. This filter weights the data to mimic human vibration sensitivity, boosting specific frequencies while limiting imperceptible low-frequency motion. This final metric acted as the validation benchmark, confirming that the numerical solution produced physically realistic results within the expected comfort zones.

## 4.0 Design Analysis

This section explores key results generated from our suspension model and the root finding procedure mentioned earlier. By adjusting the  $k_s$  and  $c_0$  values until the modal frequency and damping ratio matched targets of our design, we obtained a tuned number of suspension parameters. This section presents these values in graphical and numerical form, analyses how the system responds, and evaluates whether the behaviour of the model is realistic when compared to typical motorcycle suspension performance. This design optimizes the spring stiffness for a variety of roads, since spring stiffness optimization depends on the road type. The model was and can be edited to optimize the spring stiffness and damping coefficient to one road type, for example in the use of a race bike which is used purely on smooth road profiles. Since cobbled roads are not as common as motorways, we focussed our model more on a smooth road such as the M8. This trade-off means our system favours these smooth road profiles therefore providing more comfort when on similar roads.

## 4.1 Model Results

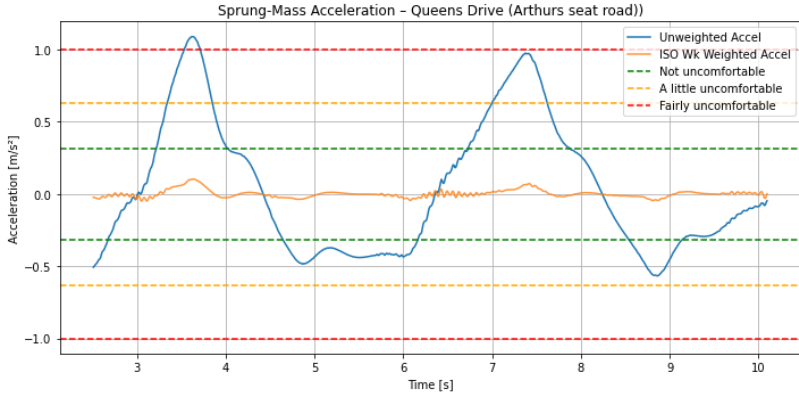


*Graph 1 - Plot showing optimal frequencies to define  $k_s$  and  $c_0$  based on their corresponding weighted rms acceleration across all roads.*

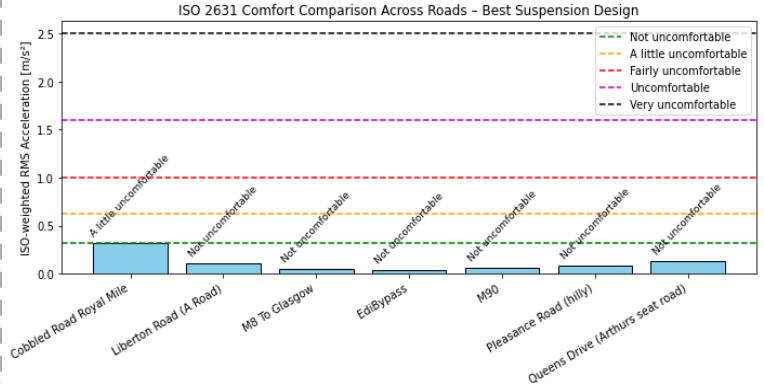
Weighted RMS Acceleration, $a_{rms}$ ( $m/s^2$ )	Optimal Stiffness $k_s$ (N/m)	Optimal Damping Coefficient, $c_0$ (Ns/m)	Frequency Target, $f$ (Hz)
0.11318	10510	508	1.45
0.11338	11333	533	1.50
0.11341	9727	483	1.40
0.11400	12197	559	1.55
0.11402	8981	460	1.35
0.11477	13105	587	1.60
0.11503	8273	437	1.30
0.11626	7601	415	1.25
0.11752	6963	394	1.20
0.11904	6358	373	1.15
0.12054	5785	353	1.10
0.12274	5244	334	1.05
0.12508	4733	315	1.00

*Table 1 – Outputs of  $a_{rms}$ ,  $k_s$  and  $c_0$ , for the target frequencies corresponding with Graph 1. The table is listed in ascending order of  $a_{rms}$ .*

Graph 1 shows that a frequency target in the range of 1.35 to 1.55 Hz yield the lowest weighted rms acceleration for our selected roads. We see that as we move the target frequency to 1 Hz, the  $a_{rms}$  increases, and therefore the comfort of the rider decreases. This led to the selection of a natural frequency of 1.45 Hz, which resulted in our optimal spring stiffness and the damping coefficient.



Graph 2- Plot of instantaneous and weighted acceleration for a candidate road: Queens Drive.



Graph 3 – Bar chart showing how the weighted acceleration of each road compares to ISO 2631 and the comfortability of each road given the chosen spring stiffness

#### 4.2 Design Decision

We assumed our scooter would be driven across a variety of roads, and therefore the analysis was performed for various road profiles. This design with **optimal stiffness ( $k_s$ ) is 10510 N/m, and corresponding damping coefficient ( $c_0$ ) of 508 Ns/m** yields the lowest weighted rms acceleration. All stiffness values analysed in the range 8980-12200 N/m gave weighted rms accelerations within 1% of this optimum with corresponding damping coefficients between 460 -560Ns/m, making alternatives in this range acceptable. These values can then be compared to values of standard springs and dampers, if the standard parts are within 10% of these values they can be used. It is optimal to use standard parts as this can cut back on manufacturing costs, allowing the scooter to be sold for a cheaper price, making it more accessible to the public.

#### 4.3 Realism and Validation of Results

To validate our results, we compared our  $c_0$ ,  $k_s$ , and natural frequency ( $\omega$ ) of the spring with values from a book on motorcycle dynamics which gave  $c_0$ ,  $k_s$ , and  $\omega$  values of 450-5400 Ns/m, 10-55 kN/m and 1.58 Hz respectively [11]. Our values all lay within these ranges so gave us confidence that our values were realistic. To confirm that our model was appropriate to the specific suspension system of the Honda PCX125, we found the rear suspension system listed in the specification of the bike [1]. The rear spring stiffness of 12-27 kN/m [15] was approximately 20% higher than our value of 10.5 kN/m. This may be due to our assumption that suspension is vertically above the wheel. As can be seen in Figure 1, the rear suspension acts at an angle to the vertical, which would mean that the vertical component of  $k_{s\text{calculated}}$  would be equal to  $(\cos\theta)k_{s\text{actual}}$ , where  $\theta$  is the angle the spring acts from vertical. As  $0 < \theta < 90^\circ$ ,  $k_{s\text{calculated}} < k_{s\text{actual}}$  perhaps suggesting why our value was outside the accepted range by approximately 20%. We are also aware that our model gives outputs directly correlating to our target of maintaining comfortable vertical acceleration, which does not represent the actual parameters that must be considered in the design of such a suspension system. For example, accelerations in other directions, static displacement of the system, and angle of impact.

The  $a_{rms}$  results exhibit trends consistent with physical expectations. From Graph 3, cobbled surfaces yielded the maximum acceleration, whereas motorways and high-speed roads resulted in the minimum values. This ordering confirms the validity of the model, demonstrating its ability to differentiate appropriately between varying road excitation levels. The optimal suspension frequency and stiffness vary significantly depending on the specific road profile. This sensitivity validates the model's realism, as ideal suspension parameters naturally depend on the dominant excitation characteristics of the surface. Furthermore, the minimal error observed between the discrete raw data points and the continuous interpolated curve confirms the high fidelity of the road profile reconstruction.

The following equations show design decision using a 1 degree of freedom system  $k = (2\pi f)^2 m = (2(\pi)(1.45))^2 (114.436125) = 9499 \frac{N}{m}$ ,  $c = 2\zeta\sqrt{km} = 2(0.2)\sqrt{(9499)(114.436125)} = 417..04 Ns/m$ . This shows that our eigenvalue analysis for the 2-DOF system yielded results in the same order of magnitude as our 1DOF analysis and validating that the optimization has not converged to an unrealistic solution.

#### 4.4 Sensitivity Analysis

% Mass Change	Optimal $k_s$ (N/m)	Optimal $c_0$ (Ns/m)	Weighted $a_{rms}$ (m/s <sup>2</sup> )	Acceptable range (N/m)	Corresponding damping range (Ns/m)
-20	8233	390	0.11313	7060-9520	355-430
+20	12886	635	0.11338	10980-15010	570-705

Table 2- Changes in optimal values when sprung mass is changed for the system.

% Tyre Stiffness Change	Optimal $k_s$ (N/m)	Optimal $c_0$ (Ns/m)	Weighted $a_{rms}$ (m/s <sup>2</sup> )	Acceptable range (N/m)	Corresponding damping range (Ns/m)
-20	10801	536	0.11373	9190-11670	480-565
+20	10325	490.2	0.11290	8850-11950	446-537

Table 3- Changes in optimal values when tyre stiffness is changed for the system.

A simple sensitivity analysis was performed by varying mass and tyre stiffness by  $\pm 20\%$  and observing the impact on key outputs. Table 2 shows that mass is highly influential in our system: lower mass decreases the optimal stiffness and damping, whilst a higher mass increases them. The trend aligns with real world vehicle dynamics as heavier vehicles require stiffer springs and higher damping to control vibrations, and lighter vehicles need a softer suspension. In Table 3, tyre stiffness is less influential, softer tyres slightly increase the optimal stiffness and damping coefficient, as would be expected to compensate for the reduced tyre support whilst stiffer tyres slightly decrease these values. The optimal suspension design remains largely within or near the acceptable range. Importantly, the trends highlights that the model outputs are physically consistent, predictable and robust across a range of vehicle configurations.

## 5.0 Conclusion

Overall, our model gives a realistic simulation of a motorcycle suspension as seen with our  $k_s$  and  $c_0$  values being similar with those implemented in the scooter. To improve our model a second system could be set up which factors in a second rider to test the optimized spring stiffness and damping coefficient. This is relevant as our end goal is to encourage the use of motorcycles as they are greener than cars, and if it's comfortable for multiple riders this could encourage ride sharing. Furthermore, given that the altitude values we received were to the nearest 0.1m, more precise data would make the model more accurate. Moreover, our model is limited to a single wheel analysis, with additional time, incorporating both wheels using a 4-DOF system for analysis could provide a more informative and accurate model. Additionally, our suspension design could be evaluated over even more road profiles to capture a larger variety of conditions. Ultimately, our objective was achieved: for majority of the road profiles, the  $a_{rms}$  values remained within the comfortable range, excluding one road which is on the border of this range. This indicates that the suspension design is robust across varying rider masses and road conditions, supporting its suitability for real-world use and reinforcing its potential to enhance comfort and encourage wider motorcycle adoption.

## 6.0 References

- [1] "PCX125 2025 Specifications," Honda UK. [Online]. Available: [https://www.honda.co.uk/motorcycles/range/scooter/pcx-125/specifications.html#model=pcx125\\_dx\\_2025&bike=pcx&colour=nh-c34m\\_matte\\_dim\\_grey\\_metallic](https://www.honda.co.uk/motorcycles/range/scooter/pcx-125/specifications.html#model=pcx125_dx_2025&bike=pcx&colour=nh-c34m_matte_dim_grey_metallic). [Accessed: Nov. 14, 2025].
- [2] D. Willigers, "Yes, motorcycles use less fuel than cars, here's the proof," FEMA, 9 May 2016. [Online]. Available: <https://www.femamotorcycling.eu/yes-motorcycles-use-less-fuel-than-cars-heres-the-proof/>. [Accessed: Nov. 14, 2025].
- [3] British Standards Institution, \*BS ISO 2631-1:1997, Mechanical vibration and shock — Evaluation of human exposure to whole-body vibration — Part 1: General requirements\*, incorporating Amendment 1:2010. London, UK: BSI, 2011. ISBN 978 0 580 66643 8.
- [4] "Top-Selling Motorbikes in the UK 2025 – New, Used, and Overall Rankings," MotoDealer, 29 Jun. 2025. [Online]. Available: <https://www.motodealer.co.uk/motorbike-news/top-selling-motorbikes-in-the-uk-2025-new-used-and-overall-rankings-1200>. [Accessed: Nov. 14, 2025].
- [5] While specific axle loads for the PCX 125 are not published, the similar Honda SH125i, which shares the same unit swingarm engine design, has an official rear-weight bias of 61.5%: Honda Motor Europe – Motorcycles, \*Scooters & 125 cc Motorcycles Brochure 2016 YM\*, Honda, London, UK. [Online]. Available: <https://www.honda.co.uk/content/dam/local/uk/brochures/motorcycles/MC%20BROCHURE%20125-SCOOTERS%20WEB%20PDF%2016YM.pdf>. [Accessed: Nov. 14, 2025].
- [6] The mean weight averages for adults in England were used as a robust proxy, as this data is not published in the equivalent Scottish Health Survey: NHS Digital, \*Health Survey for England, 2022 Part 2: Adult Overweight and Obesity\*, London, UK, Sep. 24 2024. [Online]. Available: <https://digital.nhs.uk/data-and-information/publications/statistical/health-survey-for-england/2022-part-2/adult-overweight-and-obesity>. [Accessed: Nov. 14, 2025].
- [7] The Engineering ToolBox, "Fuels – Densities and Specific Volumes," 2003. [Online]. Available: [https://www.engineeringtoolbox.com/fuels-densities-specific-volumes-d\\_166.html](https://www.engineeringtoolbox.com/fuels-densities-specific-volumes-d_166.html). [Accessed: Nov. 14, 2025].
- [8] D. J. Inman, "3 – General Forced Response," in \*Engineering Vibrations\*, Pearson Education UK, 2014, pp. 228–314. ISBN 978-0-273-76844-9.
- [9] C. F. Beards, "4 – The vibration of systems with distributed mass and elasticity," in \*Engineering Vibration Analysis with Application to Control Systems\*, C. F. Beards, Ed. Oxford, UK: Butterworth-Heinemann, 1995, pp. 141–170. ISBN 978-0-34063-183-6. doi: 10.1016/B978-034063183-6/50006-5.
- [10] C. S. Dharankar, M. K. Hada, and S. Chandel, "Performance improvement of passive suspension of vehicles using position dependent damping," \*International Journal of Vehicle Performance\*, vol. 4, no. 1, pp. 89–111, 2018. doi: 10.1504/IJVP.2018.088802.
- [11] V. Cossalter, R. Lot, and M. Massaro, "Motorcycle Dynamics," in \*Modelling, Simulation and Control of Two-Wheeled Vehicles\*, pp. 1–42, 2014. doi: 10.1002/9781118536391.ch1.
- [12] C. Deziel, "How to Convert Distances From Degrees to Meters," Sciencing, Mar. 14, 2025. [Online]. Available: <https://www.scientific.com/convert-distances-degrees-meters-7858322/>. [Accessed: Nov. 14, 2025].
- [13] E. McCarthy, "Lecture 6: Ordinary Differential Equations," \*Computational Methods and Modelling 3\*, University of Edinburgh, Sep. 2025. Lecture notes.
- [14] A. N. Rimell and N. J. Mansfield, "Design of digital filters for frequency weightings required for risk assessments of workers exposed to vibration," \*Industrial Health\*, vol. 45, no. 4, pp. 512–519, 2007. [Online]. Available: [https://www.jstage.jst.go.jp/article/indhealth/45/4/45\\_4\\_512/\\_pdf](https://www.jstage.jst.go.jp/article/indhealth/45/4/45_4_512/_pdf). [Accessed: Nov. 14, 2025].
- [15] Brook Suspension, "Honda PCX 125 YSS TG302 Twin Shock Absorbers (18-23) – Specifications," Brook Suspension, Bradford, UK. [Online]. Available: [https://www.brookssuspension.co.uk/motorcycle-shock-absorbers/honda-pcx-125-sss-tg302-twin-shock-absorbers-18-23?srsltid=AfmBOooI8N4725Duda2L5sK4vM8AHK05oZPWmG2qzKGMcLRXdm9v\\_VtB&utm](https://www.brookssuspension.co.uk/motorcycle-shock-absorbers/honda-pcx-125-sss-tg302-twin-shock-absorbers-18-23?srsltid=AfmBOooI8N4725Duda2L5sK4vM8AHK05oZPWmG2qzKGMcLRXdm9v_VtB&utm). [Accessed: Nov. 17, 2025].